Combining Two Filter Paper-Based Analytical Methods to Monitor Temporal Variations in the Geochemical Properties of Fluvial Suspended Particulate Matter

Authors: R.J. Cooper[*1], B.G. Rawlins[2], B. Lézé[1], T. Krueger[1], K.M. Hiscock[1]

[1]*School of Environmental Sciences, University of East Anglia, Norwich Research Park, Norwich, NR4 7TJ, UK*

[2]*British Geological Survey, Keyworth, Nottingham, NG12 5GG, UK*

[*] Correspondence: Richard.J.Cooper@uea.ac.uk

Abstract

Many of the commonly used analytical techniques for assessing the properties of fluvial suspended particulate matter (SPM) are neither cost-effective nor time-efficient, making them prohibitive to long-term high-resolution monitoring. We present an in-depth methodology utilising two types of spectroscopy which, when combined with automatic water samplers, can generate accurate, high-temporal resolution SPM geochemistry data, inexpensively and semi-destructively, directly from sediment covered filter papers. A combined X-ray fluorescence spectroscopy (XRFS) and diffuse reflectance infrared Fourier transform spectroscopy (DRIFTS) approach is developed to estimate concentrations for a range of elements (Al, Ca, Ce, Fe, K, Mg, Mn, Na, P, Si, Ti) and compounds (organic carbon, $Al_{dithionate}$, $Al_{oxalate}$, $Fe_{dithionate}$, and $Fe_{oxalate}$) within SPM trapped on quartz fibre filters at masses as low as 3 mg. Calibration models with small prediction errors are derived, along with mass correction factor models to account for variations in retained SPM mass. Spectral pre-processing methods are shown to enhance the reproducibility of results for some compounds, and the importance of filter paper selection and homogeneous sample preparation in minimising spectral interference is emphasized. The geochemical signal from sediment covered filter papers is demonstrated to be time stable enabling samples to be stored for several weeks prior to analysis. Example results obtained during a heavy precipitation event in October 2012, demonstrate the methodology presented here has considerable potential to be utilized for high-resolution monitoring of SPM geochemistry under a range of in-stream hydrological conditions.

Keywords: Filter Papers; Suspended Particulate Matter; Geochemistry; XRF; Infrared Spectroscopy

1. Introduction

During the past century, intensification of agriculture and extensive urbanisation have resulted in widespread sediment and nutrient enrichment of environmentally sensitive freshwater environments (Wilkinson, 2005; Cordell *et al*., 2009). Sustained high suspended particulate matter (SPM)

concentrations can cause significant fluvial degradation through the smothering of gravel salmonid spawning grounds, clogging of fish gills, elevation of turbidity, and abrasive scouring of macrophytes and periphyton (Bilotta and Brazier, 2008). SPM is also the main vector for the transport of phosphorus and other pollutants through stream systems (Russell *et al*., 1998; Bowes *et al*., 2003), and therefore enhancing our understanding of the spatial and temporal variations in SPM geochemistry is essential if sustainable ecosystem functioning is to be achieved.

Previous investigations of SPM have typically used time-integrated samplers (Phillips *et al*. 2000) as a way of obtaining sufficiently large volumes of sediment (>10 g) to facilitate detailed analysis (e.g. Panuska *et al*., 2011). However, the problem with this technique is that the SPM properties are integrated over time making them unsuitable for resolving important catchment processes (e.g. Jordan *et al*., 2007). An alternative is to use automatic water samplers that can be programmed to capture samples at defined time intervals during high-flow storm events when SPM transport is greatest (e.g. Oeurng *et al*., 2010). Unfortunately, the masses of sediment captured are often too low (<100 mg) for traditional analysis such as loss-on-ignition (LOI), colorimetry, acid digestion and Inductively Coupled Plasma (ICP), techniques which also tend to be expensive, time-consuming, and destructive. Therefore, there is a requirement for an alternative cost-effective and time-efficient technique capable of dealing with low SPM concentrations that can be used in conjunction with automatic water samplers to generate high-temporal frequency geochemistry data for a range of hydrological conditions (Evrard *et al*., 2011; Guzmán *et al*., 2013). Two candidates for this role are X-ray Fluorescence Spectroscopy (XRFS) and Diffuse Reflectance Infrared Fourier Transform Spectroscopy (DRIFTS). These spectrometers can be calibrated to directly estimate the properties of SPM trapped on filter papers with minimal prior preparation at masses as low as a few milligrams. Furthermore, because XRFS is non-destructive, it can be used in conjunction with DRIFTS on a single SPM sample to generate an array of geochemical and mineralogical data. Several studies have demonstrated the capability of XRFS (Barnhisel *et al*., 1969; Cann and Winter, 1971) and infrared spectroscopy (Martínez-Carreras *et al*., 2010a; Tremblay *et al*., 2011) to analyse SPM directly on filter papers. However, until now there has been no detailed methodology published demonstrating how the two techniques can be used consecutively to yield a wider range of high-temporal resolution geochemistry time-series. We therefore present an in-depth methodology for a combined XRFS and DRIFTS approach which considers the sensitivity of the two approaches to sediment mass retention on filter papers, methods of sample preparation, homogenisation and storage, and discusses the effects of spectral pre-processing on calibration model performance.

2. Methods

2.1 Selecting Filter Papers

69 Choosing the appropriate filter papers for spectral analysis is an important first step, since using filters

70 with a complex chemical structure will increase the risk of spectral 'noise' originating from the filter

71 paper overwhelming the signal derived from the trapped SPM. Traditionally, glass fibre filter papers

72 made from borosilicate glass are used for the laboratory filtration of stream water samples (e.g.

73 Oeurng *et al.*, 2011). However, whilst it would still be possible to use these filters after careful

74 calibration to remove background noise, we opted to use Millipore 100% quartz fibre filter (QFF)

75 papers (Merck Millipore, Billerica, MA, USA) as their simple chemistry (only Si-O bonds) generates

76 less spectral interference than typical glass fibres. These QFF papers are traditionally sold as a filter

77 for air pollution monitoring and therefore only had a particle retention rating for aerosolized Dioctyl

78 Phthanlate (DOP) particles of 99.998% at 0.3 μm. We therefore tested the average aqueous particle

79 retention by mixing 25 mg of a streambed sediment sample (Johnson *et al.*, 2005) with 1 litre of Milli-

80 Q water (18.2 MΩ.cm; Merck Millipore, Billerica, MA, USA) and vacuum filtered it through a single

81 QFF paper. This process was repeated 40 times. The resulting 40 litres of filtrate were bulked together

82 and centrifuged at 5000 rpm for 15 minutes to concentrate the colloidal particles into a 500 ml

83 solution. The concentrated filtrate was analysed in a Beckman Coulter LS13320 Laser Diffraction

84 Particle Size Analyser (Beckman Coulter, CA, USA) with 20 drops of Calgon added and 2 minutes of

85 sonication (18 W) used to disperse aggregated flocs. Total sediment mass retention was also

86 determined gravimetrically by weighing all filters after oven drying at 105°C for 2 hours.

87

88 *2.2 XRFS Calibration*

89 X-ray fluorescence spectroscopy was chosen as a method for the geochemical analysis of SPM due to

90 it being a highly accurate, non-destructive and reproducible analytical tool capable of estimating

91 concentrations of all elements from beryllium to uranium in a sample down to ppm levels (Norrish

92 and Hutton, 1969). Calibrations were made for a total of 10 major elements (Al, Ca, Fe, K, Mg, Mn,

93 Na, P, Si, Ti) and the rare earth element cerium (Ce), using 42 randomly selected, certified sediment

94 standards from various locations to form a global calibration. Cerium was selected due to it being

95 naturally enriched in phosphorus-bearing apatite minerals and therefore also being enriched in the

96 inorganic phosphate fertilizers derived from these (Land *et al.*, 1999; Reynard *et al.*, 1999). 25 mg of

97 each standard was separately mixed into suspension with 1 L of Milli-Q water in a sealed flask and

98 vacuum filtered through individual QFFs to yield 42 filter paper standards. Dispersing the sediment

99 this way ensured that each QFF had a homogeneous covering of sediment after filtering, an essential

100 step because surface roughness, uneven sediment distribution, differing densities and mixtures of

101 different particle sizes can all produce spectra that deviate from the expected theory making them

102 difficult to interpret quantitatively (Tiwari *et al.*, 2005; Maruyama *et al.*, 2008). The sediment loaded

103   filters were dried at 105°C for 2 hours before being re-weighed to determine the mass of trapped
104   sediment.

105   Each sediment covered filter paper was loaded into a wavelength-dispersive XRFS (Bruker S4
106   Pioneer, Bruker AXS, Germany) and bombarded with short wavelength X-rays for between 100-300
107   seconds per element. A blank filter paper was also loaded to provide a set of background counts at
108   each X-ray peak position that could subsequently be subtracted from counts measured on the sediment
109   covered filters. As the X-rays are emitted, some pass straight through the sample, some are back
110   scattered by Compton or Rayleigh scattering when photons collide with electrons, whilst the rest is
111   absorbed by the sediment. This absorbed fraction excites electrons within the sediment resulting in the
112   ionisation of elemental constituents by ejecting one or multiple electrons from the inner K- and L-
113   orbitals. This destabilises the electron structure causing the outer shells to collapse inwards filling in
114   the vacancy left by the ejected electrons. The transition of electrons from higher to lower energy
115   atomic shells releases X-ray fluorescence radiation with wavelengths and energies characteristic of
116   the orbitals involved and the atoms present within the sample (Bruker, 2008). These fluorescence
117   spectra were recorded and a mathematical 'peak search' technique was employed to find spectral
118   peaks, whilst a 'peak match' procedure determined the elements to which each peak belongs by
119   referring to a database of reference values (Brouwer, 2003).

120   Of the 42 prepared standards, 26 were used to develop the calibration model which took the general
121   form (Brouwer, 2003):

122   *(1)* $C_x = (A_x + B_x * I_x) * M_x / MCF$

123   where C_x is the estimated concentration of element x, A_x and B_x are the gradient and intercept
124   determined by linear regression from the reference standards, and I_x is the measured intensity. M_x is
125   the matrix correction factor which corrects for various effects that impact upon the number of photons
126   being ejected from a sample (Enzweiler and Vendemiatto, 2004). These include the partial elemental
127   absorption of X-rays attenuating the resulting fluorescent emission, as well as the enhancement of
128   emission spectra by fluorescent X-rays of heavy elements stimulating further secondary fluorescence
129   of lighter elements. Further corrections for Compton matrix scattering and spectral peak line overlaps
130   (deconvolutions) were applied using the Bruker S4 Pioneer software, reviewed in more detail in
131   Brouwer (2003). MCF is the mass correction factor which accounts for the inability to obtain exactly
132   25 mg of SPM (the calibration mass) on each filter paper every time a stream water sample is filtered.
133   Barnhisel *et al*. (1969) and Cann and Winter (1971) previously demonstrated that individual mass
134   correction adjustments are required for each element because the XRFS procedure assumes all
135   samples are of equal mass. Therefore, deviations between the mass of SPM retained and the mass
136   used for calibration will strongly impact upon elemental concentrations predicted by XRFS.
137   Individual MCFs were developed for each element by dividing the estimated percentage concentration

4

138 of four reference standards at a range of masses (3-60 mg) by the percentage concentration at the

139 calibration mass (Equation 2):

140 *(2)* $MCF = C_x / C_{xCM}$

141 where C_x is the estimated concentration of element *x* at any given mass, and C_{xCM} is the concentration

142 of element *x* at calibration mass (i.e. 25 mg). This yields MCF fractions with values <1 for sediment

143 masses below 25 mg and >1 for masses higher than 25 mg. A regression model was then formulated

144 to explain the relationship between the MCF and sediment mass, from which adjustments can be

145 made to the estimated concentration by dividing by the appropriate MCF value (Equation 1).

146 Calibrations were subsequently verified against the remaining 16 independent standards using an

147 iterative predictive model that works by first predicting element *n=1*, then *n=1, 2*, and so on

148 continuously up to *n=11*, with the final iteration taken as the elemental composition of the sample as

149 this accounts for all of the various aforementioned matrix interactions between each element

150 (Brouwer, 2003).

151

152 *2.3 DRIFTS Calibration*

153 *2.3.1 Sample Selection*

154 Alongside XRFS, diffuse reflectance infrared Fourier transform spectroscopy (DRIFTS) is proposed

155 as a complementary, semi-destructive, analytical technique capable of determining concentrations of

156 various compounds present within SPM. Covalently bonded molecules have a characteristic

157 rotational-vibrational structure unique to the mass of the atoms and strength of the bonding between

158 them. DRIFTS exploits this by targeting a beam of multi-frequency mid-infrared (4000-400 cm^{-1})

159 light onto a ground SPM sample, where upon infrared light that matches the resonant frequency of the

160 molecular bonds is absorbed producing a characteristic absorption spectrum at a specific wavelength

161 unique to the vibrational frequency of that particular bond. The remainder of the light is either

162 reflected or refracted, with only the diffusely reflected fraction utilised in the DRIFTS procedure

163 (Tremblay and Gagné, 2002).

164 Numerous studies have already demonstrated the effectiveness of infrared spectroscopy in the

165 geochemical analysis of both soils (Viscarra Rossel *et al.*, 2006; Rawlins, 2011b; Stumpe *et al.*, 2011)

166 and stream sediments (Poulenard *et al.*, 2009 & 2012; Martínez-Carreras *et al.*, 2010a,b; Rawlins,

167 2011a). The advantage here being it can be used directly on SPM covered filter papers after the

168 elemental composition has been derived by XRFS. Calibrations were made for a total of 5 compounds

169 (organic carbon, $Al_{dithionate}$, $Al_{oxalate}$, $Fe_{dithionate}$, and $Fe_{oxalate}$) selected based on the well documented

170 organo-mineral associations that occur within soils and stream sediments (e.g. Evans *et al.*, 2004;

171 Wagai *et al*., 2009; Hartikainen *et al*., 2010). However, in contrast to XRFS, which can be accurately

172 calibrated using globally derived certified standards, Minasny *et al.* (2009) demonstrated that the

173 regional transferability of mid-infrared spectra measurements is relatively weak. Therefore, local

174 calibrations had to be derived using a selection of 92 dry ground soils (Rawlins, 2011b) and

175 streambed sediment samples (Johnson *et al*., 2005) from the River Blackwater catchment in Norfolk,

176 UK (52°47$^{'}$N, 1°07'E). This site was chosen as part of a wider Department for Environment, Food and

177 Rural Affairs (DEFRA) funded River Wensum Demonstration Test Catchment initiative (Wensum

178 Alliance, 2012), which aims to investigate how on-farm mitigation measures can reduce diffuse water

179 pollution whilst maintaining food production capacity. Because the soil types within the catchment

180 range from sandy and chalky boulder clays in the west, to sands and gravels in the east (Rawlins,

181 2011b), a reasonable degree of geochemical and mineralogical variability was provided for

182 calibration.

183 Organic carbon (OC) contents for each calibration sample were derived gravimetrically following

184 combustion of 1 g of dry ground sediment at 450°C for 8 hours, with OC taken to be 58% of the LOI

185 (Broadbent, 1953). Crystalline Fe and Al oxyhydroxides concentrations were determined via

186 dithionite extraction (McKeague and Day, 1966) by weighing out 1 g of sediment into a 30 ml

187 centrifuge tube along with 20 ml of 25% (w/v) sodium citrate ($Na_3C_6H_5O_7.2H_2O$) and 5 ml of 10%

188 (w/v) sodium dithionite (NaS_2O_4) before shaking overnight. Samples were centrifuged at 2500 rpm

189 for 20 minutes before a 15 ml aliquot of the supernatant was extracted and filtered through a 0.45 μm

190 Whatman membrane syringe filter prior to ICP-AES analysis to determine the concentrations of

191 dithionate extractable iron (Fe_{di}) and aluminium (Al_{di}). Amorphous iron and aluminium mineral phase

192 concentrations were determined via oxalate extraction by adding 25 ml of ammonium oxalate (0.2 M;

193 $C_2H_8N_2O_4$) and oxalic acid ($H_2C_2O_4$ – 15.76 g l^{-1}) to 1.5 g of sediment in a centrifuge tube. The

194 resulting mixture was shaken for 2 hours and processed as for the dithionite extraction to yield

195 concentrations of oxalate extractable iron (Fe_{ox}) and aluminium (Al_{ox}).

196

197 *2.3.2 Sample Preparation*

198 Once OC and oxyhydroxide concentrations had been determined for all 92 calibration samples, 25 mg

199 of each sample was transferred onto individual QFF papers using the same procedure as for the XRFS

200 calibration. Unlike infrared transparent potassium bromide (KBr), which is traditionally used as the

201 sole background matrix for DRIFTS analysis not on filter papers, quartz fibres produce strong

202 absorption features in the region 1200-1000 cm^{-1} (Masserschmidt *et al*., 1999). This can reduce

203 infrared beam penetration depth to as little as 10 μm meaning only sediment at the sample cup surface

204 will be analysed and spectral band intensities will be suppressed. Consequently, the way in which the

205 absorbing matrix material is prepared will affect the degree of scatter, the amount of Fresnel

reflectance, and the interaction between sediment and infrared radiation making it easy to misinterpret changes in the spectra due to matrix effects as genuine changes in the sediment chemical composition (Brimmer and Griffiths, 1986). There were therefore four key preparation factors that had to be considered in order to obtain good quality reproducible spectra with a high degree of interpretational accuracy (Pike Technologies, 2011):

1- **Particle size**: large particles >50 μm result in major Fresnel reflection off particle surfaces which increases scattering and yields noisy spectra with wide bandwidths and low absorption intensities (Brimmer and Griffiths, 1986).

2- **Packing**: samples were loosely and evenly packed into cups every time to both maximise infrared beam penetration and to minimise spectral distortions and irregularities caused by Fresnel reflections off compacted sample surfaces.

3- **Grinding**: the degree of grinding can affect spectral properties by destroying chemical bonds and thereby reducing the specific light absorption of those molecules (Stumpe *et al*., 2011).

4- **Homogeneity**: spectra from non-homogeneous samples will be severely affected by matrix scattering causing spectra to lose crucial reproducibility and making them difficult to quantitatively interpret.

With these points in mind, each sediment covered filter was uniformly ground for 50 seconds into a fine homogeneous powder using a ShakIR steel ball mill (Pike Technologies, Madison, WI, USA). A small amount of KBr was added to act as an infrared transmitting matrix and an effective abrasive agent helping to reduce particle sizes. The resulting powders were lightly hand packed into steel sample cup holders and scanned 40 times at 4 cm^{-1} resolution across the wave-number range 4000-400 cm^{-1} in a BIO-RAD Excalibur Series FTS-3000 FTIR (Cambridge, MA, USA) fitted with an AutoDiff^{TM} automated diffuse reflectance accessory (Pike Technologies, Madison, WI, USA). Sample cups were rotated through 90° after the first scan and rescanned another 40 times so that spectra could be averaged to offset any potential spectral reflectance noise generated by the orientation of the powdered particles. A background spectrum of the QFF and KBr matrix was also collected and subtracted from all subsequent sample scans to isolate the sediment signal using the Resolutions Pro spectral processing software (Agilent Technologies, CA, USA).

2.3.3 Chemometrics

Having carefully prepared and scanned all samples, a multivariate partial least squares (PLS) regression model with leave-one-out (LOO) cross-validation was developed using the '*pls*' package (Mevik *et al*., 2011) in the *R* environment (R Development Core Team, 2012). Such multivariate model calibration is beneficial over univariate regression as the wavelength at which the signal is

240 present does not have to be generated exclusively by the target compound. Instead, PLS regression
241 models exploit the fact that different compounds have different absorbance at a range of wavelengths
242 which can then be used to decipher information from multiple overlapping spectral bands without
243 prior band assignment (Alaoui *et al*., 2011). Because concentration estimates derived from DRIFTS
244 are a reflection of the relative proportion of ground SPM to filter paper within the sample cup, mass
245 correction factors again had to be developed in the same way as for XRFS.

246

247 *2.3.4 Spectral Pre-processing*

248 A potential limitation of using DRIFTS on filter papers is the inability to obtain highly reproducible
249 spectra when considerable noise is generated from the quartz fibre matrix. Four methods of spectral
250 pre-processing were therefore assessed to determine whether applying certain filters or corrections
251 prior to developing the PLS regression would enhance model strength, and more specifically, whether
252 it would enhance the reproducibility of the resulting concentration estimates. These four methods
253 were: i) no pre-processing, ii) mean centring and 15 point first order Savitzky-Golay filtering
254 (Savitzky and Golay, 1964; Martínez-Carreras *et al*., 2010a), iii) Multiplicative Scatter Correction
255 (MSC), and iv) mean centring, filtering, and MSC (Figure 1). Savitzky-Golay filtering was applied
256 using the '*signal*' package in *R* (Short, 2011) to reduce high frequency variations associated with
257 matrix noise whilst still preserving the line shape and lower frequency trends associated with the
258 sediment signal. Prior to applying the low-pass filter, the spectra were mean centred such that they all
259 had a common baseline, thereby removing any potential drift effects of the spectrometer. MSC was
260 applied using the '*pls*' package which, theoretically, distinguishes between and separates absorption
261 features of the actual sediment from the random light-scattering noise generated by the background
262 matrix (Martens *et al*., 2003).

263

264 *2.4 Temporal Degradation*

265 An advantage of utilising both XRFS and DRIFTS directly on filter papers is that, once dried, large
266 numbers of samples from automatic samplers can be stored for an extended period of time prior to
267 analysis, thereby removing the need for analytical facilities to be immediately available once the
268 stream water samples have been returned to the laboratory. Whilst it is known that oven dried
269 sediment samples can be stored for many months, or even years, prior to elemental analysis without
270 degrading (e.g. USEPA, 2001), we decided to test whether this remains the case when only a few
271 milligrams of sediment is distributed across a filter paper. The reason being that a small mass of
272 sediment exposed on the relatively large surface area of the filter paper could make the samples more

273   susceptible to biological or chemical degradation than traditionally stored bulk sediment samples with

274   a lower surface area to mass ratio. For XRFS, this was tested by re-analysing three of the calibration

275   standards at 39, 68, 80, 94, 109 and 122 days since the filters were initially prepared. The results for

276   the three standards were then averaged together and the concentrations expressed relative to the day

277   the standards were prepared. During this time, the oven dried sediment-covered filters were

278   individually stored at room temperature in a sealed air-tight box with silica gel desiccant beads. For

279   DRIFTS it was not possible to re-analyse the initial calibration samples as, once ground, the resulting

280   powders readily absorb water which alters the resulting spectra. As such, two new calibration samples

281   were prepared at 49, 42, 29, 22 and 4 days prior to DRIFTS analysis. The results where then averaged

282   to offset any variability in concentration estimates arising from slight differences in the preparation of

283   the ten new standards. Once prepared, these standards were stored in a dark cupboard at room

284   temperature in individual air-tight plastic bags.

285

3. Results and Discussion

287   *3.1 Filter Papers*

288   The bulked particle size distribution of the filtrate revealed an average aqueous particle retention

289   rating of 99.26% at 0.45 µm (99.04% at 0.7 µm) for the forty QFF papers (Figure 2), with an average

290   mass retention of $94.5 \pm 5.2\%$. This confirms the suitability of these filters for SPM investigation with

291   respect to their ability to retain nearly all clay and silt-sized fractions from suspension. Importantly,

292   this includes particulates at 0.7 µm, operationally defined as the threshold between SPM (0.7-63 µm)

293   and dissolved constituents (<0.7 µm), as well at 0.45 µm which marks the transition between

294   dissolved and particulate P fractions. Very fine colloidal material (1-100 nm) may still pass through,

295   although as the pores become blocked by larger particles, retention of colloids will be enhanced.

296

297   *3.2 XRFS*

298   The XRFS calibration results are displayed in Figure 3 as the actual versus predicted percentage

299   concentrations of all 11 elements. Of the 26 prepared calibration standards, a few provided weak

300   correlations and were therefore rejected from the final regression model. In most cases, rejected

301   standards had either visibly uneven sediment distribution or poor sediment retention (i.e. filters had

302   retained less than 25 mg of sediment), with some elements (e.g. Fe) more affected by this

303   inhomogeneity in sample preparation than others. All calibrations, derived from between 13 to 25

304   standards, are statistically significant ($P<0.001$) with adjusted variance explained statistics ranging

305   from 93.4% for Si to 99.7% for K (Table 1). All validation estimates are also statistically significant

306   (p<0.001), with adjusted variance explained statistics ranging from 63.9% for Si to 95.9% for Ca. The

307   weaker validation shown for Si arises from the imperfect removal of the silicon-rich QFF paper

308   background, and as such, caution needs to be exercised when using the Si data. As is typical with

309   regressions of this type, the uncertainty around the calibration increases towards the upper end of the

310   concentration range where there are fewer reference standards, particularly for both Mn and P where

311   validation samples deviate substantially from expected values. Despite this, the 95% confidence

312   intervals are relatively narrow and the majority of the validation samples fall within a small range of

313   the calibration line.

314   For the mass correction factors (MCFs), strong, positive logarithmic (Al, Mg, Na, P) and power law

315   (Ca, Ce, Fe, K, Ti) relationships were established for 9 out of 11 elements, being strongest for Ca (R^2

316    $= 0.992$) and weakest for Ce ($R^2 = 0.934$) (Figure 4). The non-linearity between sediment mass and

317   the MCF arises because as the sediment mass on the filter paper increases, the intensity of fluorescent

318   X-ray generation from each element per milligram of sediment declines due to an increasing influence

319   of matrix attenuation. As such, increases in sediment at small masses have a greater impact on

320   fluorescent X-ray generation than an increase in sediment at large masses. In contrast, Si exhibits a

321   strong negative logarithmic relationship with increasing sediment mass which reflects the fact that

322   smaller sediment masses are associated with increased X-ray penetration depth and therefore

323   enhanced fluorescence generation originating from the QFF. For Mn, the relationship between

324   sediment mass and the MCF is much weaker and best fitted by a linear relationship. It is not clear why

325   the Mn MCF regression performs poorly by comparison with the other elements, but it may relate to

326   stronger matrix interactions with other elements. The results demonstrate that variations in SPM mass

327   can be corrected by simple regression models.

328

329   *3.3 DRIFTS*

330   The impact of applying various spectral pre-processing techniques to the DRIFTS spectra can be seen

331   in Figure 5, which shows the concentration estimates for OC, Al_{di}, and Fe_{di} in six batches of the same

332   sediment standard. No plots are shown for either Al_{ox} or Fe_{ox} as these exhibited near identical patterns

333   to Al_{di} and Fe_{di} respectively. Both no pre-processing (NPP) and mean centring and Savitzky-Golay

334   filtering (MCSG) methods yield significantly higher reproducibility than multiplicative scatter

335   correction (MSC) or a combination of all methods (ALL). Whilst several authors have used MSC as a

336   pre-processing tool in infrared spectroscopy (e.g. Vogel *et al*., 2008; Martínez-Carreras *et al*., 2010),

337   the simplicity of the technique means that it can erroneously remove spectral signals derived from the

338   sediment chemical bonds, thereby yielding poorly representative spectra that worsen the multivariate

339   model calibration, as has occurred here. For both OC, and in particular the iron compounds, MCSG

340   yields higher reproducibility and was therefore chosen as the spectral pre-processing method for these

compounds. For both Al_{di} and Al_{ox}, there was little difference in the performance of NPP and MCSG, however NPP yielded a stronger calibration model (lower root mean squared error of prediction (RMSEP)), negating the need to pre-process the spectra for aluminium compounds. Also shown is the reproducibility of spectra prepared by hand grinding the filter papers in an agate pestle and mortar as opposed to the ShakIR ball mill. The wide variability in concentration estimates emphasises the importance of producing homogeneously ground and mixed sample powders prior to analysis if precise results are to be obtained, something that manual hand grinding is unable to achieve.

The DRIFT model calibrations are displayed (Figure 6) as measured versus predicted concentrations for OC, Al_{di}, Al_{ox}, Fe_{di}, and Fe_{ox} with leave-one-out cross validation. Rather than allow the PLS model to be run over the full spectrum (4000-400 cm^{-1}), discrete spectral regions were selected for each compound to enhance model calibrations. For OC (3975-1300 cm^{-1}) this included a very strong absorption feature in a band around 2950-2845 cm^{-1} caused by symmetric and asymmetric stretching and vibration of various aliphatic and aromatic C-H bonds, as well as bands around 1300-1125 cm^{-1} associated with ester, ether and phenol groups, and at 2035-1975 cm^{-1} due to aromatic rings (Alaoui *et al.*, 2011; Tremblay *et al.*, 2011). For Fe_{di} (3704-3189 cm^{-1}) and Fe_{ox} (1727-1320 cm^{-1}) this included numerous absorption features in the regions 2500-1666 cm^{-1} and 3800-3200 cm^{-1} associated with iron bearing minerals such as hematite, maghemite, lepidocrocite, goethite, and magnetite (Namduri and Nasrazandani, 2008). For Al_{di} (3903-2202 cm^{-1}) and Al_{ox} (3849-2879 cm^{-1}) the major absorption features occur in a band around 3800-3200 cm^{-1} associated with the stretching of O-H bonds in aluminosilicates (Tremblay *et al.*, 2011). Although other relevant absorption features are known to occur in the region 1200-400 cm^{-1}, this band was avoided because it is dominated by matrix noise from the QFF that make quantitative interpretation impossible. The optimum number of principal model components selected for each calibration (n= 7-10) was based on the lowest achievable RMSEP following leave-one-out cross-validation. All five calibrations are statistically significant, with variance explained statistics for the cross-validated models ranging from 74.6% for Al_{ox} to 96.6% for OC (Table 2). However, the limited number of high Fe_{di} and Fe_{ox} concentration standards does increase model uncertainly at larger concentrations.

Strong linear regression MCF models with narrow confidence intervals have been developed for OC ($R^2 = 0.935$), Al_{di} ($R^2 = 0.918$), Fe_{di} ($R^2 = 0.925$) and Fe_{ox} ($R^2 = 0.884$) (Figure 7). As with the XRFS, uncertainty increases towards the extremes of the concentration range. A weaker association was established between Al_{ox} and sediment mass ($R^2 = 0.860$) that is best fitted by a power law relationship. This likely arises due to the weaker PLS calibration model derived for Al_{ox}, and as such, there is greater uncertainty in adjusting for retained SPM mass. Despite this, the strong regression models developed here demonstrate the ability of the DRIFTS MCF values to adjust for fluctuating in-stream SPM concentrations.

376

3.4 Temporal Stability

Relative concentrations for the XRFS standards vary by less than 5% for all elements expect Mn during the 122-day period over which they were analysed (Figure 8). This level of variability is within the range of the calibration uncertainty, which, along with the absence of any apparent temporal trends in the data, strongly suggests the filter paper standards do not degrade over time. The largest amount of temporal variability occurs for Ce and P, although this reflects small changes in the estimated actual concentration of these low abundance elements (Ce = ~0.0062% and P = ~0.068%) having a comparatively large impact on their estimated relative concentrations. For DRIFTS, relative concentrations vary by less than 8.5% during the 49-day period over which they were analysed, with no longer term trends apparent in the data. Although temporal variability is greater than observed for the XRFS, it is within the range of calibration uncertainty. The higher DRIFTS variability also reflects the fact that the same calibration samples are not being analysed each time, and as such, some noise is introduced by sample preparation. We can therefore conclude that once oven dried at 105°C for 2 hours, sediment covered filters can be reliably stored at room temperature in an air-tight environment for several months without risk of degradation.

3.5 Example Application

The effectiveness of these two techniques is demonstrated using data from a heavy precipitation event in October 2012 within the 20 km^{2} lowland, intensive arable, River Blackwater catchment, Norfolk (Figure 9). ISCO automatic water samplers (Teledyne ISCO, Lincoln, NE) were activated to sample 1 litre of water every hour for 24 hours at the beginning of a 10 hour period during which 10.6 mm of precipitation was recorded. The storm event is characterised by increases in the concentrations of SPM, clay associated elements (e.g. Al, Fe, Mg, K), and organic carbon, coupled with a sharp decline in the concentration of calcium. These changes in geochemistry, which begin ~6 hours after the onset of precipitation, occur approximately concurrently with the rise in stage. As the rainfall event ends these trends reverse, with declines in stage, clay associated elements and OC combined with increases in calcium. These temporal patterns in geochemistry reflect spatial changes in SPM source areas within the catchment. The catchment geology is characterised by the Upper Cretaceous Chalk formation overlain by sandy and chalky boulder clays of the Quaternary Sheringham Cliffs Formation which become less weathered with depth. Before and after the event, SPM is rich in calcium indicating sediment is predominantly derived from the deeper less-weathered subsoils exposed in eroded stream channel banks. In contrast, during heavy rainfall, the generation of overland flow, particularly from road runoff, carries large quantities of highly weathered, calcium-depleted, clay-rich

410 topsoil into the stream. The identification of these temporal fluctuations in SPM geochemistry
411 exemplifies the advantage of using a combined XRFS/DRIFTS technique with automatic water
412 samplers, as such results would be impossible to obtain using time-integrated samplers. Note, the
413 apparent large uncertainties around Mg and Na measurements are a reflection of the low
414 concentrations of these elements in the River Blackwater relative to the calibration standards.

415

416 *3.6 Experimental Limitations*

417 Despite the strong calibration results for both XRFS and DRIFTS, there are limitations to analysing
418 SPM geochemistry directly on filter papers. Principally, when using time-integrated samplers, a
419 sufficiently large mass of SPM (>10g) can be captured, sieved and fractionated, thereby enabling the
420 importance of the colloidal, clay, silt and sand fractions, as well as algal and detrital material, to be
421 assessed independently. Clearly, when analysing masses of 25 mg in-situ on filter papers such size
422 fractionation is impossible. However, given that the majority of SPM is <63 μm in diameter
423 (averaging 86% by volume in the River Blackwater under both high and low flow conditions), this is
424 not a major analytical limitation. Additionally, unlike XRFS which is a truly non-destructive
425 analytical technique, the DRIFTS procedure outlined here is best described as semi-destructive.
426 Whilst the grinding of SPM covered QFFs does not affect the chemistry of the sample, which can still
427 be analysed by other laboratory methods, the fact that it is now in powdered form does prevent the
428 samples from being reanalysed by XRFS using the same procedure. Finally, in selecting DRIFTS
429 standards spatially restricted to the River Blackwater catchment, the resulting calibrations are
430 regionally specific to this particular lowland intensive arable environment. To apply this technique
431 further afield would require the addition of samples from catchments local to the study region
432 (Minasny *et al.*, 2009).

433

434 **4. Conclusions**

435 Many commonly used methods for determining the properties of suspended particulate matter (SPM),
436 both in the field (e.g. time-integrated samplers) and in the laboratory (e.g. ICP, LOI), are neither cost-
437 effective nor time-efficient, making them prohibitive for long-term high-resolution monitoring. We
438 have demonstrated an alternative method using two types of spectroscopy applied directly to sediment
439 covered filter papers to quickly generate accurate geochemistry data without altering the SPM
440 chemistry. By utilising a combination of XRFS and DRIFTS, it is possible to obtain concentration
441 estimates for a range of elements (Al, Ca, Ce, Fe, K, Mg, Mn, Na, P, Si, Ti) and compounds (organic
442 carbon, Al_{di}, Al_{ox}, Fe_{di}, and Fe_{ox}) from a single SPM covered filter paper at masses as low as a few

milligrams, thereby removing the requirement for the collection of large sample volumes in the field. When combined with automatic water samplers, large numbers of SPM covered filter paper discs can be cheaply produced via simple vacuum filtering, thereby enabling hydrologically dynamic storm events to be monitored in high-resolution. We have demonstrated that QFF papers are appropriate for this type of analysis by minimising spectral interference and retaining nearly all SPM greater than 0.45 μm. Homogeneous sample preparation was shown to be essential if accurate and reproducible results are to be obtained, whilst local DRIFTS calibration is necessary for the technique to be applied in other catchments due to the weak regional transferability of mid-infrared spectra measurements. Pre-processing the infrared spectra by mean centring and Savitzky-Golay filtering prior to developing PLS regression models proved to be the most effective way to generate reproducible concentration estimates for both OC and iron oxyhydroxide complexes, whilst aluminium compounds did not require processing. The development of property-specific mass correction factor (MCF) models enables variations in retained SPM mass from that used during calibration to be corrected for by simple regression. The temporal stability of filter paper standards prepared up to 122 days prior to analysis indicates that it is possible to store batches of sediment covered filters for several months if necessary. The example application presented here demonstrates considerable potential for a combined XRFS and DRIFTS approach to be used in conjunction with automatic water samplers as a tool for the high-resolution analysis of SPM geochemistry in a range of fluvial systems.

References

Alaoui G, Léger MN, Gagné J-P, Tremblay L. 2011. Assessment of estuarine sediment and sedimentary organic matter properties by infrared reflectance spectroscopy. *Chemical Geology* **286**: 290-300. DOI: 10.1016/j.chemgeo.2011.05.012

Barnhisel RI, Phillippe WR, Blevins RL. 1969. A simple X-ray fluorescence technique for the determination of iron and manganese in soils and concretion. *Soil Science Society of America Proceedings* **33**: 811-813.

Bilotta GS, Brazier RE. 2008. Understanding the influence of suspended solids on water quality and aquatic biota. *Water Research* **42**: 2849-2861. DOI: 10.1016/j.watres.2008.03.018.

477 Bowes MJ, House WA, Hodgkinson RA. 2003. Phosphorus dynamics along a river continuum. *Science of the*
478   *Total Environment* **313**: 119–212. DOI: 10.1016/S0048-9697(03)00260-2.
479
480 Brimmer PJ, Griffiths PR. 1986. Effect of absorbing matrices on diffuse reflectance infrared spectra. *Analytical*
481   *Chemistry* **58**: 2179-2184. DOI: 10.1021/ac00124a015.
482
483 Broadbent FE. 1953. The soil organic fraction. *Advances in Agronomy* **5**: 153-183.
484
485 Brouwer P. 2003. Theory of XRF: Getting acquainted with the principles. PANalytical BV: Almelo,
486   Netherlands; 10-66.
487
488 Bruker. 2008. S4 Pioneer Spectrometry Solutions. Bruker AXS GmbH: Karlsruhe, Germany; 4-8.
489 Cann JR, Winter CK. 1971. X-ray fluorescence analysis of suspended sediment in sea water. *Marine Geology*
490   **11**: 33-37. DOI: 10.1016/0025-3227(71)90002-8.
491
492 Cordell D, Drangert J-O, White S. 2009. The story of phosphorus: Global food security and food for thought.
493   *Global Environmental Change* **19**: 292-305. DOI: 10.1016/j.gloenvcha.2008.10.009.
494 Enzweiler J, Vendemiatto MA. 2004. Analysis of sediments and soils by X-ray fluorescence spectrometry using
495   matrix corrections based on fundamental parameters. *Geostandards and Geoanalytical Research* **28**:
496   103-112. DOI: 10.1111/j.1751-908X.2004.tb01046.x.
497
498 Evans DJ, Johnes PJ, Lawrence DS. 2004. Physico-chemical controls on phosphorus cycling in two lowland
499   streams. Part 2 – The sediment phase. *Science of the Total Environment* **329**: 165-182. DOI:
500   10.1016/j.scitotenv.2004.02.023.
501
502 Evrard O, Navratil O, Ayrault S, Ahmadi M, Némery J, Legout C, Lefèvre I, Poirel A, Bonté P, Esteves M.
503   2011. Combining suspended sediment monitoring and fingerprinting to determine the spatial origin of
504   fine sediment in a mountainous river catchment. *Earth Surface Processes and Landforms* **36**: 1072-
505   1089. DOI: 10.1002/esp.2133.
506
507 Guzmán G, Quinton JN, Nearing MA, Mabit L, Gómez JA. 2013. Sediment tracers in water erosion studies:
508   current approaches and challenges. *Journal of Soils and Sediments* **13**, 816-833. DOI: 10.1007/s11368-
509   013-0659-5.
510
511 Hartikainen H, Rasa K, Withers PJA. 2010. Phosphorus exchange properties of European soils and sediments
512   derived from them. *European Journal of Soil Science* **6**: 1033-1042. DOI: 10.1111/j.1365-
513   2389.2010.01295.x. DOI: 10.1111/j.1365-2389.2010.01295.x.
514 Johnson CC, Breward N, Ander EL, Ault L. 2005. G-BASE: baseline geochemical mapping of Great Britain and
515   Northern Ireland. *Geochemistry: Exploration, Environment, Analysis* **5**: 347-357. DOI: 10.1144/1467-
516   7873/05-070.
517
518 Jordan P, Arnscheidt A, McGrogan H, McCormick, S. 2007. Characterising phosphorus transfers in rural
519   catchments using a continuous bank-side analyser. *Hydrology and Earth System Science* **11**: 372–381.
520
521 Land M, Öhlander B, Ingri J, Thunberg J. 1999. Solid speciation and fractionation of rare earth elements in a
522   spodosol profile from northern Sweden as revealed by sequential extraction. *Chemical Geology* **160**:
523   121-138. DOI: 10.1016/S0009-2541(99)00064-9.

524   Martens H, Nielsen JP, Engelsen SB. 2003. Light scatting and light absorbance separated by extended
525   multiplicative signal correction. Application to near-infrared transmission analysis of powder mixtures.
526   *Analytical Chemistry* **75**: 394-404. DOI: 10.1021/ac020194w.

527   Martínez-Carreras N, Krein A, Udelhoven T, Gallart F, Iffly JF, Hoffmann L, Pfister L, Walling DE. 2010a. A
528   rapid spectral-reflectance-based fingerprinting approach for documenting suspended sediment sources
529   during storm runoff events. *Journal of Soils and Sediments* **10**: 400-413. DOI: 10.1007/s11368-009-
530   0162-1.

531   Martínez-Carreras N, Udelhoven T, Krein A, Gallart F, Iffly JF, Ziebel J, Hoffmann L, Pfister L, Walling DE.
532   2010b. The use of sediment colour measured by diffuse reflectance spectrometry to determine sediment
533   sources: Application to the Attert River catchment (Luxembourg). *Journal of Hydrology* **382**: 49-63.
534   DOI: 10.1016/j.jhydrol.2009.12.017.

535   Maruyama Y, Ogawa K, Okada T, Kato M. 2008. Laboratory experiments of particle size effect in X-ray
536   fluorescence and implications to remote X-ray spectrometry of lunar regolith surface. *Earth, Planets
537   and Space* **60**: 293-297.

538   Masserschmidt I, Cuelbas CJ, Poppi RJ, De Andrade JC, De Abreu CA, Davanzo CU. 1999. Determination of
539   organic matter in soils by FTIR/Diffuse reflectance and multivariate calibration. *Journal of
540   Chemometrics* **13**: 265-273. DOI: 10.1002/(SICI)1099-128X(199905/08)13:3/4<265::AID-
541   CEM552>3.3.CO;2-5.

542   McKeague JA, Day JH. 1966. Dithionite- and oxalate-extractable Fe and Al as aids in differentiating various
543   classes of soils. *Canadian Journal of Soil Science* **46**: 13-22. DOI: 10.4141/cjss66-003.

544   Mevik B-J, Wehrens R, Liland KH. 2011. R Package: *'pls'*: Partial Least Squares and Principal Component
545   regression.

547   Minasny B, Tranter G, McBratney AB, Brough DM, Murphy BW. 2009. Regional transferability of mid-
548   infrared diffuse reflectance spectroscopic prediction for soil chemical properties. *Geoderma* **153**: 155-
549   162. DOI: 10.1016/j.geoderma.2009.07.021

551   Namduri H, Nasrazadani S. 2008. Quantitative analysis of iron oxides using Fourier transform infrared
552   spectrophotometry. *Corrosion Science* **50**: 2493-2497. DOI: 10.1016/j.corsci.2008.06.034.

553   Norrish K, Hutton JT. 1969. An accurate X-ray spectrographic method for the analysis of a wide range of
554   geological samples. *Geochimica et Cosmochimica Acta* **33**: 431-453. DOI: 10.1016/0016-
555   7037(69)90126-4.

557   Oeurng C, Sauvage S, Sánchez-Pérez JM. 2010. Dynamics of suspended sediment transport and yield in a large
558   agricultural catchment, southwest France. *Earth Surface Processes and Landforms* **35**: 1289-1301.
559   DOI: 10.1002/esp.1971.

561   Oeurng C, Sauvage S, Coynel A, Maneux E, Etcheber H, Sánchez-Péez J-M. 2011. Fluvial transport of
562   suspended sediments and organic matter during flood events in a large agricultural catchment in
563   southwest France. *Hydrological Processes* **25**: 2365-2378. DOI: 10.1002/hyp.7999.

565   Panuska JC, Good LW, Vadas PA, Busch DL, Ozkaynak A. 2011. Sediment and particulate phosphorus
566   characteristics in grassed waterways from row crop corn and alfalfa fields collected by manual
567   University of Exeter samplers and automatic sampling. *Hydrological Processes* **25**: 2329-2338. DOI:
568   10.1002/hyp.7987.

569 Phillips JM, Russell MA, Walling DE. 2000. Time-integrated sampling of fluvial suspended sediment: a simple
570   methodology for small catchments. *Hydrological Processes* **14**: 2589-2602. DOI: 10.1002/1099-
571   1085(20001015)14:14<2589::AID-HYP94>3.0.CO;2-D

572 Pike Technologies. 2011. Diffuse Reflectance – Theory and Applications. Madison, USA; 39-40.
573

574 Poulenard J, Perrette Y, Fanget B, Quetin P, Trevisan D, Dorioz JM. 2009. Infrared spectroscopy tracing of
575   sediment sources in a small rural watershed (French Alps). *Science of the Total Environment* **407**:
576   2808-2819. DOI: 10.1016/j.scitotenv.2008.12.049.

577 Poulenard J, Legout C, Némery J, Bramorski J, Navratil O, Douchin A, Fanget B, Perrette Y, Evrard O, Esteves
578   M. 2012. Tracing sediment sources during floods using Diffuse Reflectance Infrared Fourier Transform
579   Spectrometry (DRIFTS): A case study in a highly erosive mountainous catchment (Southern French
580   Alps). *Journal of Hydrology* **414-415**: 452-462. DOI: 10.1016/j.jhydrol.2011.11.022.

581 R Development Core Team. 2012. R: A language and environment for statistical computing. R Foundation for
582   Statistical Computing: Vienna, Austria. http://www.R-project.org.
583

584 Rawlins BG. 2011a. Controls on the phosphorus content of fine stream bed sediment in agricultural headwater
585   catchments at the landscape scale. *Agriculture, Ecosystems and Environment* **144**: 352-363**.** DOI:
586   10.1016/j.agee.2011.10.002.

587 Rawlins BG. 2011b. A pilot study to assess soil spectroscopic methods for mapping key topsoil properties in the
588   Blackwater sub-catchments (Wensum DTC). British Geological Survey, Climate Change Programme,
589   Internal Report OR/11/053; 1-19.

590 Reynard B, Lécuyer C. Grandjean P. 1999. Crystal-chemical controls on rare-earth element concentrations in
591   fossil biogenic apatites and implications for paleoenvironmental reconstructions. *Chemical Geology*
592   **155**: 233-241. DOI: 10.1016/S0009-2541(98)00169-7.

593 Russell MA, Walling DE, Webb BW, Bearne R. 1998. The composition of nutrient fluxes from contrasting UK
594   river basins. *Hydrological Processes* **12**: 1461-1482. DOI: 10.1002/(SICI)1099-
595   1085(199807)12:9<1461::AID-HYP650>3.0.CO;2-6

596 Savitzky A, Golay MJ. 1964. Smoothing and differentiation of data by simplified least square procedures.
597   *Analytical Chemistry* **36**: 1627–1639. DOI: 10.1021/ac60214a047.

598 Short T. 2011. R Package *'signal'*: Signal Processing.
599

600 Stumpe B, Weihermullerm L, Marschner B. 2011. Sample preparation and selection for qualitative and
601   quantitative analyses of soil organic carbon with mid-infrared reflectance spectroscopy. *European*
602   *Journal of Soil Science* **62**: 849-862. DOI: 10.1111/j.1365-2389.2011.01401.x

603 Tiwari MK, Singh AK, Sawhney KJS. 2005. Sample preparation for evaluation of detection limits in X-ray
604   florescence spectrometry. *Analytical Sciences* **21**: 143-147. DOI: 10.2116/analsci.21.143.

605 Tremblay L, Alaoui G, Léger MN. 2011. Characterization of aquatic particles by direct FT-IR analysis of filters
606   and quantification of elemental and molecular compositions. *Environment, Science, and Technology*
607   **45**: 9671-9679. DOI: 10.1021/ac011043g.

608 USEPA. 2001. Methods for Collection, Storage and Manipulation of Sediments for Chemical and Toxicological
609   Analyses: Technical Manual. EPA 823-B-01-002. U.S. Environmental Protection Agency, Office of
610   Water, Washington, DC; 1-16.

611 Viscarra Rossel RA, Walvoort DJJ, McBrantney AB, Janik LJ, Skjemstad JO. 2006. Visible, near infrared, mid
612   infrared or combined diffuse reflectance spectroscopy for simultaneous assessment of various soil
613   properties. *Geoderma* **131**: 59-75. DOI: 10.1016/j.geoderma.2005.03.007.

615 Vogel H, Rosén P, Wagner B, Melles M, Persson P. 2008. Fourier transform infrared spectroscopy, a new cost-
616   effective tool for quantitative analysis of biogeochemical properties in long sediment records. *Journal*
617   *of Paleolimnology* **40**: 689-702. DOI: 10.1007/s10933-008-9193-7.

619 Wagai R, Mayer LM, Kitayama K. 2009. Extent and nature of organic coverage of soil mineral surfaces
620   assessed by a gas sorption approach. *Geoderma* **149**: 152-160. DOI: 10.1016/j.geoderma.2008.11.032.

622 Wensum Alliance. 2012. River Wensum Demonstration Test Catchment Project. Online:
623   www.wensumalliance.org.uk

625 Wilkinson BH. 2005. Humans as geologic agents: A deep-time perspective. *Geology* **33**: 161-164. DOI:
626   10.1130/G21108.1.

627
628
629
630
631
632
633
634
635
636
637
638
639
640
641
642
643
644
645
646
647
648
649
650
651
652
653
654
655
656
657
658
659
660
661
662

TABLES:

Table 1: Summary XRFS calibration and validation statistics for the percentage concentration of 11 elements (Al, Ca, Ce, Fe, K, Mg, Mn, Na, P, Si, Ti) in 42 certified sediment standards determined directly on filter papers. *n* standards refer to the fraction of available standards used. SE is the standard error

Element	Calibration			Validation			
	n standards	Adjusted R^2	SE (%)	*n* standards	Adjusted R^2	SE (%)	*P*-value
Al	22/26	0.971	0.494	16/16	0.941	1.290	$3.5e^{-10}$
Ca	25/26	0.996	0.418	16/16	0.959	0.627	$2.2e^{-11}$
Ce	24/26	0.966	0.001	14/16	0.901	0.001	$1.3e^{-7}$
Fe	13/26	0.994	0.264	16/16	0.923	0.943	$2.1e^{-9}$
K	25/26	0.997	0.106	16/16	0.958	0.479	$3.0e^{11}$
Mg	19/26	0.988	0.345	15/16	0.707	0.320	$5.1e^{-5}$
Mn	22/26	0.951	0.019	14/16	0.749	0.076	$3.8e^{-5}$
Na	20/26	0.985	0.143	16/16	0.978	0.196	$3.1e^{-13}$
P	22/26	0.947	0.012	15/16	0.818	0.073	$2.2e^{-6}$
Si	18/26	0.934	2.128	16/16	0.639	3.564	$1.2e^{-4}$
Ti	16/26	0.996	0.038	16/16	0.840	0.097	$3.6e^{-7}$

Table 2: Summary DRIFTS partial least squares regression statistics for concentrations of organic carbon, Al_{di}, Al_{ox}, Fe_{di}, and Fe_{ox} in calibration samples determined directly on filter papers. *n* PCs are the number of principle components selected, RMSEP is the Root Mean Square Error of Prediction, MC is mean centred, and SG is Savitzky-Golay smoothed.

Compound	*n* standards	Pre-processing	Spectral Region (cm^{-1})	*n* PCs	Calibration R^2	Calibration RMSEP	Validation R^2	Validation RMSEP
Organic Carbon (%)	50	MC, SG	3975-1300	10	0.990	0.326	0.966	0.589
Al_{di} (mg/kg)	59	None	3903-2202	10	0.978	67.46	0.842	179.97
Al_{ox} (mg/kg)	62	None	3849-2879	10	0.993	33.79	0.746	211.51
Fe_{di} (mg/kg)	57	MC, SG	3704-3189	10	0.971	970.20	0.893	1865.10
Fe_{ox} (mg/kg)	51	MC, SG	1727-1320	7	0.945	536.90	0.823	956.90

FIGURES:
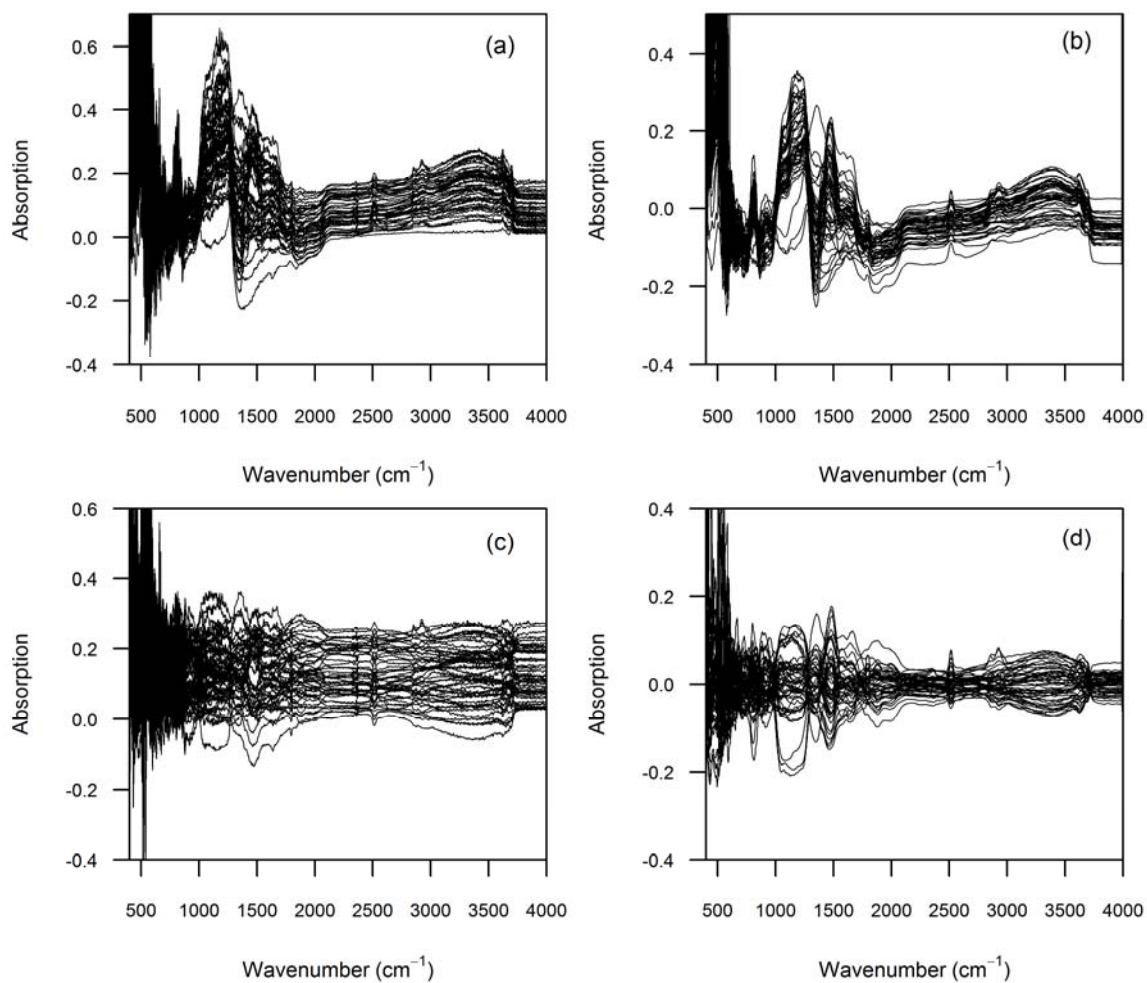
684

Figure 1: Mid-infrared (4000-400 cm-1) DRIFT spectra for 92 River Blackwater catchment standards showing

the impact of various spectral pre-processing methods on the resulting spectral shape. (a) No pre-processing; (b)

mean centred and Savitzky-Golay smoothed; (c) multiplicative scatter corrected; (d) multiplicative scatter

corrected, mean centred, and Savitzky-Golay smoothed.

689

690

691
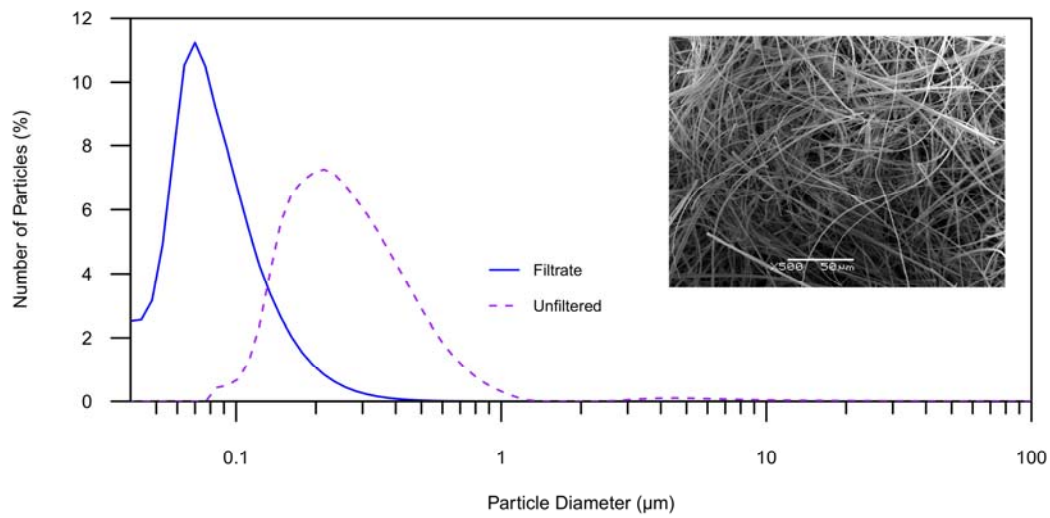
Figure 2: Average particle size distribution of the Millipore quartz fibre filtrate, shown alongside the unfiltered streambed sediment sample. Inset shows a scanning electron microscope (SEM) image of a Millipore quartz fibre filter paper at 500 times magnification, highlighting the random structure of the quartz fibres.

696
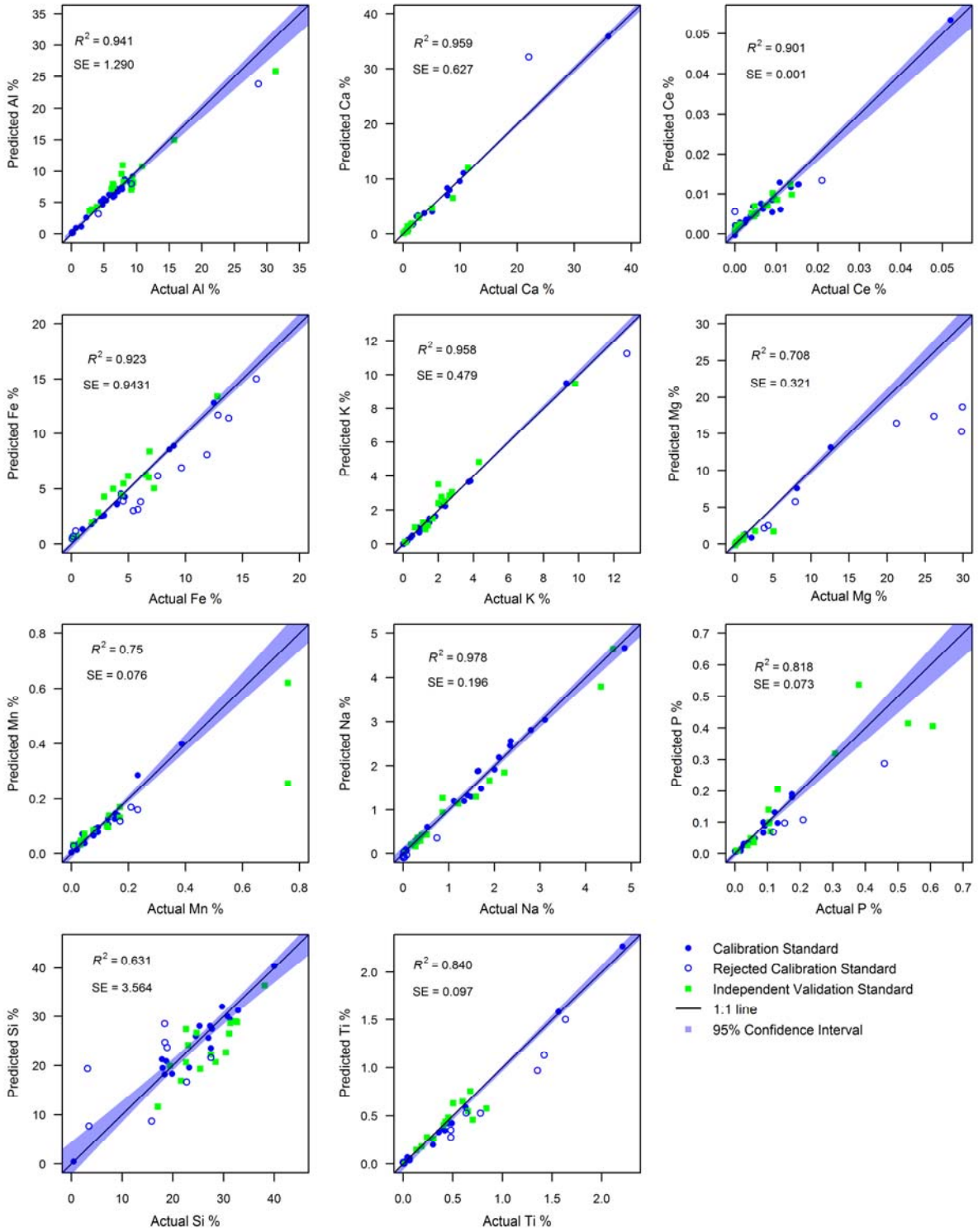
Figure 3: XRFS calibration and validation plots for the percentage concentration of 11 elements (Al, Ca, Ce, Fe,
K, Mg, Mn, Na, P, Si, Ti) in 42 sediment standards. 95% confidence intervals refer to the regression calibration.
Adjusted R^2 and standard error (SE) statistics refer to the validation dataset.
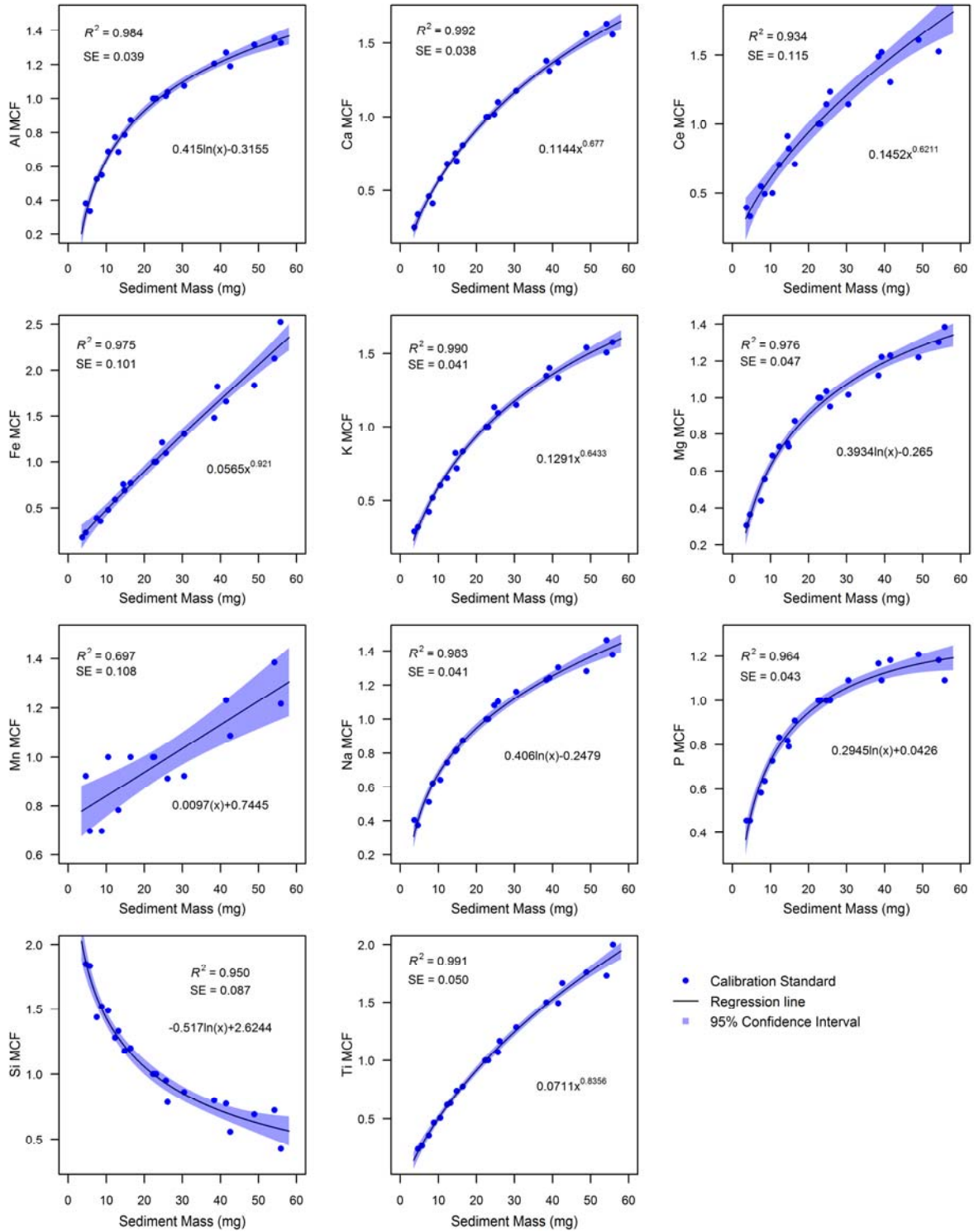
703

704   Figure 4: XRFS mass correction factor (MCF) calibration plots for 11 elements (Al, Ca, Ce, Fe, K, Mg, Mn, Na,

705   P, Si, Ti) in four certified sediment standards of varying mass.

706

707
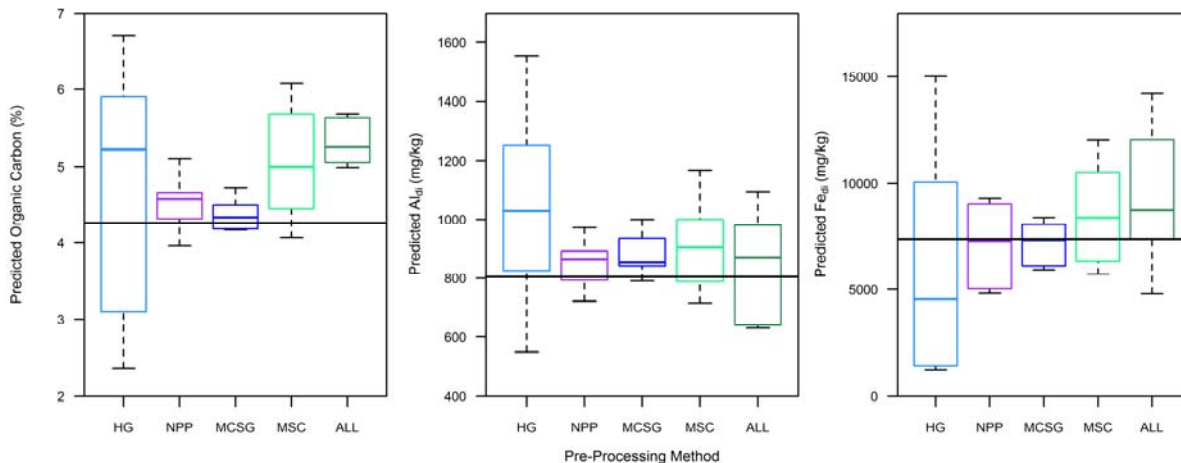
Figure 5: Box-plots demonstrating the impact of various DRIFTS spectral pre-processing methods on the reproducibility of concentration estimates for organic carbon, Al_{di}, and Fe_{di} in six batches of a calibration sample. HG are hand ground samples with no pre-processing; the others are ShakIR ball mill ground samples, whereby NPP is no pre-processing; MCSG is mean centred and Savitzky-Golay filtered; MSC is multiplicative scatter correction; ALL is MCSG and MSC combined. The solid black line is the measured concentration in the calibration sample, the solid line at the centre of the box is the median, the top and bottom of the boxes represent the interquartile range, and the whiskers are the maximum and minimum values.
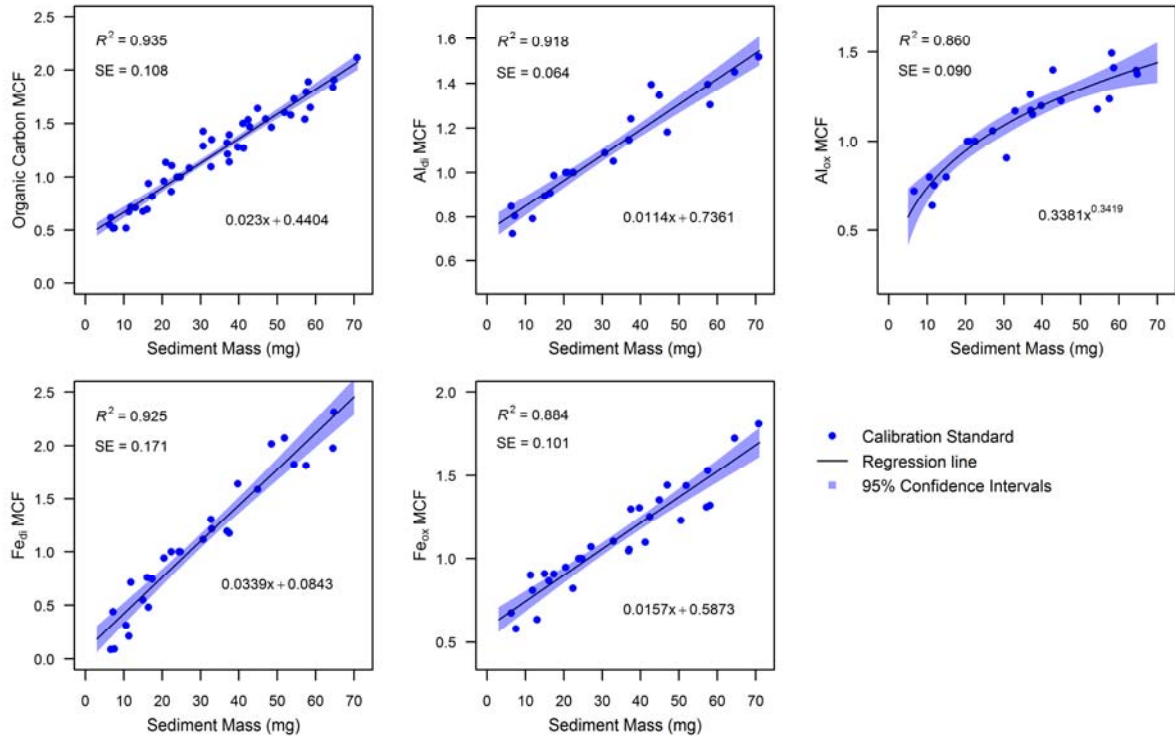

717
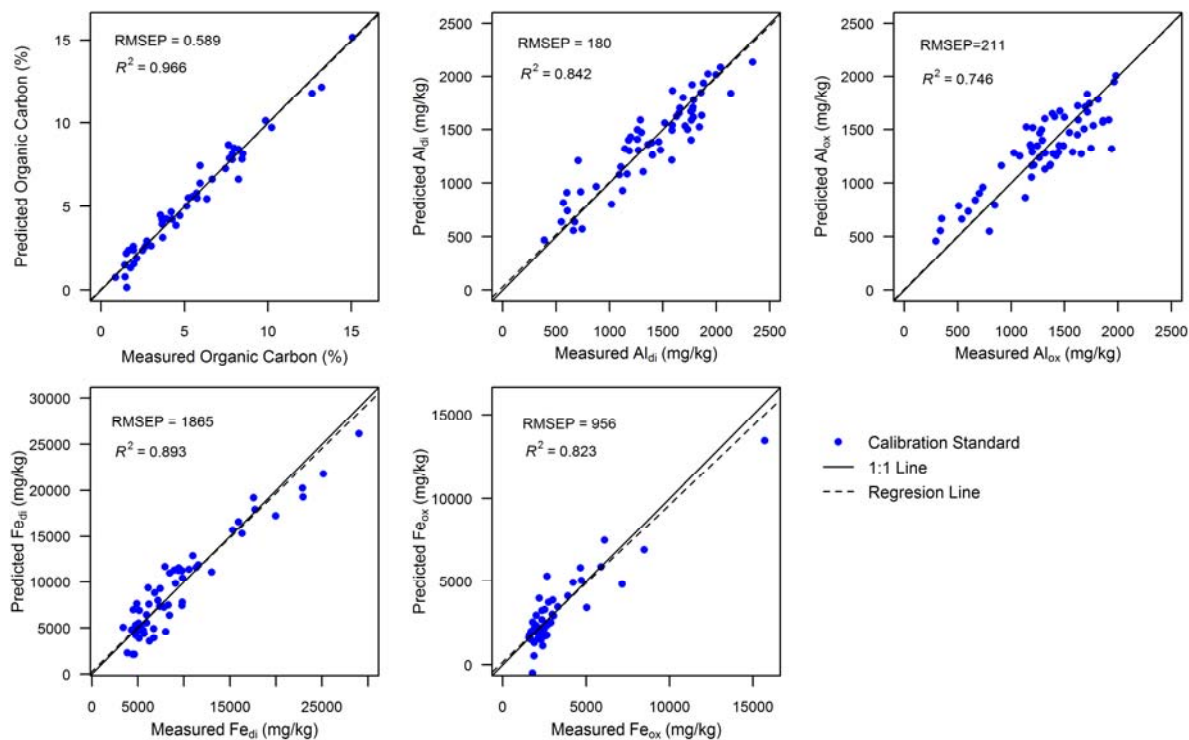
Figure 6: DRIFTS partial least squares calibration plots with leave-one-out (LOO) cross validation for organic carbon, Al_{di}, Al_{ox}, Fe_{di}, and Fe_{ox}.
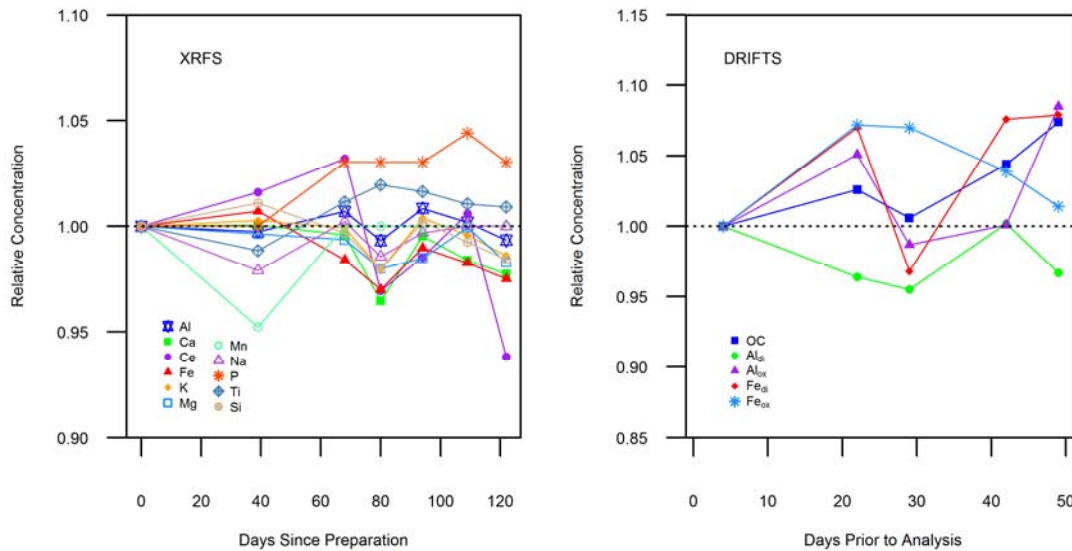
24

720

721 Figure 7: DRIFTS mass correction factor (MCF) calibration plots for five compounds (organic carbon, Al_{di},

722 Al_{ox}, Fe_{di}, Fe_{ox}) in four calibration samples of varying mass.

723

724

725

726 Figure 8: Time series plots showing the relative geochemical concentrations in 16 calibration samples against
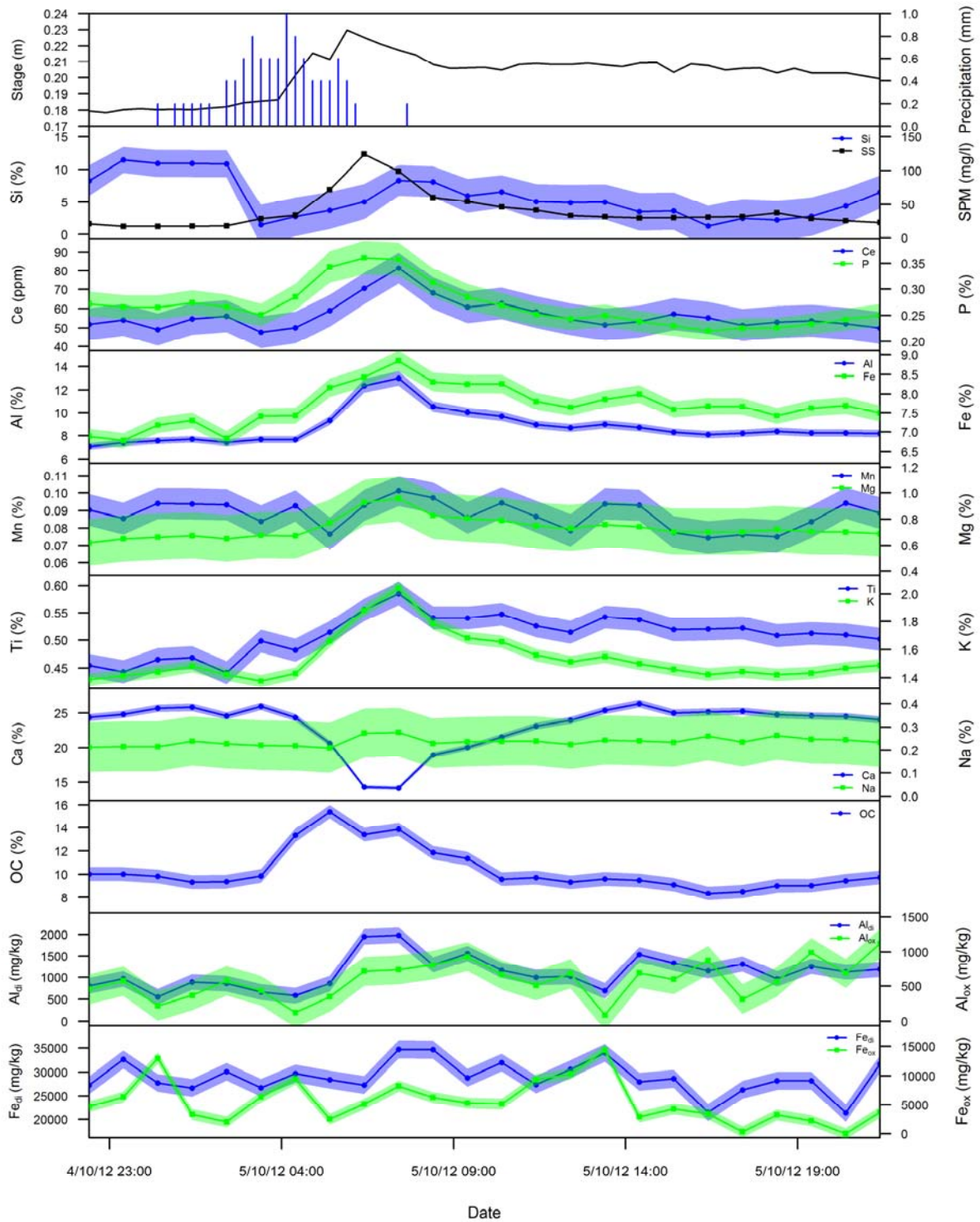
727 the number of days between filter paper preparation and analysis. XRFS concentrations are expressed relative to

728 the day the filter paper standards were prepared, whilst DRIFTS concentrations are expressed against filter

729 paper standards prepared four days prior to analysis.

730

731

732

Figure 9: Time series plot demonstrating the effectiveness of the XRFS and DRIFTS procedures in monitoring
the temporal variability of SPM geochemistry in the River Blackwater during a heavy rainfall event in October
2012. Points relate to the times automatic water samplers captured samples. Shading represents the 95%
confidence intervals based on calibration uncertainty.